ejpmr, 2025, 12(4), 633-643

SJIF Impact Factor 7.065

EUROPEAN JOURNAL OF PHARMACEUTICAL AND MEDICAL RESEARCH

www.ejpmr.com

Research Article

ISSN 2394-3211

EJPMR

PREPARATION AND CHARACTERIZATION OF CHITOSAN-BASED NANOPARTICLES OF ATOVAQUONE

Shivanjali Jejurkar*[1], Khushal Chavan[1], Prof. Bhushan P. Wagh[2]

[1]M. Pharm (Pharmaceutics) Students, Department of Pharmaceutics, Mahatma Gandhi Vidyamandir's Pharmacy College, Panchavati, Nashik-422003, India.

[2]Professor, Department of Pharmaceutics, Mahatma Gandhi Vidyamandir's Pharmacy College, Panchavati, Nashik-422003, India.

***Corresponding Author: Shivanjali Jejurkar**

M. Pharm (Pharmaceutics) Students, Department of Pharmaceutics, Mahatma Gandhi Vidyamandir's Pharmacy College, Panchavati, Nashik-422003, India.

Article Received on 22/02/2025 **Article Revised on 14/03/2025** **Article Published on 04/04/2025**

ABSTRACT

This study focuses on the preparation and characterization of chitosan-based nanoparticles of Atovaquone (ATQ-NPs) to enhance its solubility and bioavailability. Atovaquone, a poorly water-soluble drug, faces challenges in achieving effective therapeutic concentrations. To overcome this limitation, ionic gelation was employed to formulate chitosan nanoparticles as a drug delivery system. The ATQ-NPs were synthesized using chitosan and sodium tripolyphosphate (TPP) as crosslinkers, optimizing particle size and stability. The nanoparticles were characterized using Fourier-transform infrared spectroscopy (FTIR), differential scanning calorimetry (DSC), scanning electron microscopy (SEM), dynamic light scattering (DLS), and zeta potential analysis. The optimized formulation exhibited a particle size of 271 nm, polydispersity index (PDI) of 0.521, and a zeta potential of +30.5 mV, indicating good stability. Encapsulation efficiency and drug loading capacity were determined as 83.87% and 16.69%, respectively. In vitro drug release studies revealed a sustained release pattern in simulated gastric and intestinal fluids, with release kinetics following a zero-order model. The results suggest that ATQ-NPs significantly enhance drug solubility and provide controlled release, potentially improving therapeutic efficacy.) In conclusion, chitosan-based nanoparticles offer a promising strategy for Atovaquone delivery, addressing solubility and bioavailability concerns. These findings pave the way for further in vivo studies and potential clinical applications in the treatment of parasitic infections.

KEYWORDS: Atovaquone, Chitosan nanoparticles, Ionic gelation, Drug delivery, Sustained release.

1. INTRODUCTION

Nanotechnology has revolutionized the field of pharmaceutical sciences, offering novel approaches for drug delivery and therapeutic enhancement.[1] Among these, nanoparticles have gained significant attention due to their ability to improve the solubility, stability, and bioavailability of poorly water-soluble drugs.[2] By reducing particle size to the nanometer range (1-100 nm), nanoparticles provide a larger surface area, allowing for improved drug dissolution and absorption.[3] Moreover, their controlled and targeted drug release properties help in minimizing side effects while maximizing therapeutic efficacy.[4] Various polymeric nanoparticles, such as chitosan, polylactic acid (PLA), and poly(lactic-co-glycolic acid) (PLGA), have been extensively studied as drug carriers due to their biodegradability and biocompatibility.[5] In particular, chitosan-based nanoparticles have emerged as an excellent platform for delivering poorly soluble drugs, making them a promising strategy in modern drug delivery systems.[6]

Atovaquone (ATQ) is a highly lipophilic antiprotozoal drug primarily used in the treatment and prevention of malaria and Pneumocystis pneumonia (PCP).[7] It acts by selectively inhibiting the mitochondrial electron transport chain, specifically targeting cytochrome bc1 complex in the respiratory pathway of Plasmodium falciparum and Pneumocystis jirovecii, thereby disrupting ATP synthesis and leading to parasite death.[8] Due to its broad-spectrum activity, Atovaquone is often prescribed in combination with proguanil hydrochloride (marketed as Malarone®) for malaria prophylaxis and with sulfamethoxazole-trimethoprim (TMP-SMX) alternatives for PCP treatment in immunocompromised patients.[9] Despite its effectiveness, Atovaquone suffers from poor aqueous solubility (less than 0.2 µg/mL in water) and low oral bioavailability (~23%), which significantly limits its therapeutic potential.[10] The high hydrophobicity of Atovaquone leads to erratic absorption in the gastrointestinal (GI) tract, resulting in variable plasma concentrations and reduced efficacy.[11] Furthermore, its poor permeability and hepatic

metabolism contribute to inconsistent drug levels, necessitating high oral doses to achieve therapeutic effects.[12] Overcoming these limitations is crucial for enhancing the clinical performance of Atovaquone, making nanotechnology-based drug delivery systems a promising approach to improve its solubility, bioavailability, and therapeutic efficiency.[13]

Chitosan, a biocompatible and biodegradable polysaccharide derived from chitin, has gained significant attention in nanoparticle-based drug delivery due to its unique physicochemical properties.[14] It is water-soluble in acidic environments, possesses mucoadhesive properties, and has a cationic nature that facilitates interaction with negatively charged biological membranes.[15] These properties make chitosan-based nanoparticles (CS-NPs) a promising vehicle for enhancing drug solubility, improving bioavailability, and enabling sustained drug release.[16] Additionally, CS-NPs protect drugs from enzymatic degradation, enhancing stability and prolonging circulation time.[17] For hydrophobic drugs like Atovaquone, chitosan nanoparticles offer a dual advantage: they can encapsulate poorly water-soluble drugs and improve their aqueous solubility while ensuring targeted delivery.[18] Studies have shown that chitosan-based nanocarriers significantly enhance the oral absorption of lipophilic drugs, making them an ideal choice for overcoming Atovaquone's solubility limitations.[19]

Several techniques have been developed for the formulation of nanoparticles, each with distinct advantages and limitations.[20] Some of the widely used methods include emulsification, precipitation, and ionic gelation. The emulsification technique involves dispersing the drug in a polymeric solution followed by solvent evaporation, but it often requires toxic organic solvents.[21] The precipitation method relies on rapid solvent exchange, leading to uncontrolled particle growth and aggregation.[22] Ionic gelation, on the other hand, is a solvent-free, simple, and scalable process that enables efficient nanoparticle synthesis at room temperature.[23] For this study, ionic gelation was chosen due to its biocompatibility, ease of preparation, and ability to produce stable nanoparticles with controlled drug release properties.[24] This method involves the electrostatic interaction between positively charged chitosan and negatively charged crosslinkers such as sodium tripolyphosphate (TPP), leading to nanoparticle formation without the need for high shear forces or organic solvents.[25] This makes it an ideal approach for encapsulating Atovaquone, ensuring enhanced solubility, stability, and bioavailability.

The present study aims to develop ”nd characterize chitosan-based nanoparticles (CS-NPs) of Atovaquone to enhance its solubility, improve bioavailability, and enable sustained drug release.[26] Given Atovaquone's poor aqueous solubility and low oral bioavailability, the ionic gelation method was selected to formulate a stable nanoparticulate system for effective drug delivery.[27] To assess the physicochemical properties and performance of the formulated nanoparticles, various characterization techniques were employed, including:

- Fourier-transform infrared spectroscopy (FTIR): To confirm drug-polymer interactions.[28]
- Differential scanning calorimetry (DSC): To determine drug crystallinity and thermal behaviour.[29]
- Scanning electron microscopy (SEM): To analyze particle size and surface morphology.[30]
- Dynamic light scattering (DLS) and zeta potential analysis: To evaluate particle size distribution, stability, and surface charge.
- In vitro drug release studies: To investigate drug release kinetics in simulated gastric and intestinal fluids.

By developing chitosan-based nanoparticles, this study aims to offer an efficient drug delivery platform that enhances Atovaquone's solubility, stability, and therapeutic potential, paving the way for its clinical application in malaria and Pneumocystis pneumonia treatment.

2. MATERIALS AND METHODS

2.1 Materials

Atovaquone (gift sample) was obtained from Glenmark Pharmaceuticals, Mumbai, while chitosan and sodium tripolyphosphate (TPP) were sourced from Research-Lab Fine Chem Industries and Akshar Exim Co. Pvt. Ltd., respectively. Other analytical-grade chemicals were procured from Modern Science Labs Pvt. Ltd. Formulation and characterization were performed using a Remi magnetic stirrer (2 MLH), Chemito UV-Vis spectrophotometer, Shimadzu FT-IR spectrometer, Malvern Zetasizer, and Brookhaven SEM. Drug release studies utilized Dialysis Membrane 50 (Dolphin Instrument Pvt. Ltd.).

2.2. Methods

Atovaquone-loaded chitosan nanoparticles (ATQ-NPs) were prepared using the ionic gelation method. Chitosan (1% w/v- 2%w/v) was dissolved in 1% v/v acetic acid under continuous stirring, while sodium tripolyphosphate (TPP) solution (0.5% w/v- 2%w/v) was prepared separately in distilled water. The TPP solution was added dropwise to the chitosan solution under constant stirring (2,000 rpm), allowing nanoparticle formation through electrostatic interaction. The resulting suspension was stirred for 2 hours, followed by centrifugation at 10,000 rpm for 30 minutes to collect the nanoparticles. The obtained ATQ-NPs were washed with distilled water, freeze-dried, and stored at 4°C for further analysis.

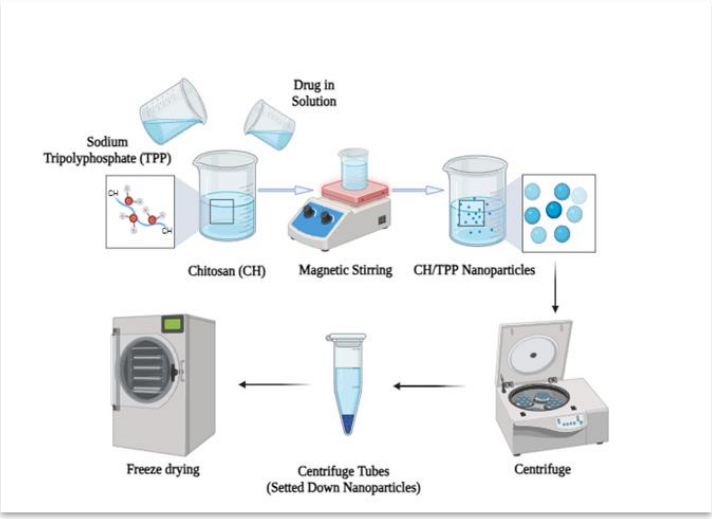

Figure 1: Graphical Method of Preparation of ATQ-NPs.

2.3. Optimization of ATQ-NPs

Based on the results of preliminary experiments, the **ATQ-NPs** was optimized by Box–Behnken design with two factors and three responses. The design of experiments and statistical analysis was conducted by Design Expert® 13 software (Stat-Ease Inc, Minneapolis, MN, USA). Atovaquone (API) (X1), Chitosan (Polymer) (X2) were chosen as factors. In addition, particle size (Y1), polydispersity index (Y2), and encapsulation efficiency (Y3) of **ATQ-NPs** were selected as responses to optimize the **ATQ-NPs**. Thirteen of the designed experiments were conducted, and the resulting responses were fitted to linear, cubic, quadratic, special cubic, or quadratic polynomial models. To optimize the fitting model for each response, various statistical parameters, such as sequential p-values, lack of fit, squared correlation coefficient (R2), adjusted R2, and adequate precision were considered by comparing various statistical parameters provided by analyses of variance (ANOVA). After fitting the statistical model, the desirability value according to the goal of responses was obtained by numerical optimization and the **ATQ-NPs** with the highest desirability value was prepared as the selected composition. A recovery test was performed to compare the error between the predicted and actual values.

Table I: Parameters of Experimental Design.

Factors	Range	
	Low Limit	High Limit
X1: Atovaquone (API)	50 mg	200 mg
X2: Chitosan (Polymer)	100 mg	200 mg
Response	**Goal**	
Y1: Particle size (nm)	Minimize	
Y2: Polydispersity index	Minimize	
Y3: Encapsulation efficiency (%)	Maximize	

Table II: Formulation Batches of ATQ-NPs.

	Factor 1	Factor 2
Batches	A:API (mg)	B:Chitosan (mg)
ATQ-NPs 1	125	150
ATQ-NPs 2	18.934	150
ATQ-NPs 3	125	150
ATQ-NPs 4	125	79.2893
ATQ-NPs 5	125	220.711
ATQ-NPs 6	125	150
ATQ-NPs 7	200	100
ATQ-NPs 8	200	200
ATQ-NPs 9	125	150
ATQ-NPs 10	231.066	150
ATQ-NPs 11	50	200
ATQ-NPs 12	50	100
ATQ-NPs 13	125	150

3. Characterization of Atovaquone-Loaded Chitosan Nanoparticles (ATQ-NPs)

3.1. Particle Size, Polydispersity Index (PDI), and Zeta Potential

The particle size, polydispersity index (PDI), and surface charge (zeta potential) of ATQ-NPs were determined using Dynamic Light Scattering (DLS). These parameters play a crucial role in nanoparticle stability, drug release, and bioavailability. A Malvern Zetasizer (Malvern Instruments, UK) was used for analysis, and measurements were taken in aqueous dispersion at 25°C. The PDI value indicates the uniformity of particle distribution, where a lower PDI suggests a more homogeneous nanoparticle population.

Table III: Particle size (Y1) and Polydispersity Index (Y2) of Formulations ATQ-NPs1-13.

Batches	Particle Size	Polydispersity Index
ATQ-NPs 1	176.5 ± 2.25	0.182 ± 0.0012
ATQ-NPs 2	182.4 ± 3.18	0.236 ± 0.0015
ATQ-NPs 3	203.6 ± 1.46	0.556 ± 0.0025
ATQ-NPs 4	284.7 ± 0.87	0.252 ± 0.0095
ATQ-NPs 5	176.5 ± 3.25	0.182 ± 0.0096
ATQ-NPs 6	299.6 ± 1.18	0.533 ± 0.0026
ATQ-NPs 7	430.3 ± 1.55	0.472 ± 0.0045
ATQ-NPs 8	704.1 ± 3.31	0.955 ± 0.0065
ATQ-NPs 9	266.1 ±3.36	0.456 ± 0.0056
ATQ-NPs 10	708.3 ± 1.55	0.922 ± 0.0035
ATQ-NPs 11	461.8 ±2.90	0.823 ± 0.0045
ATQ-NPs 12	501.5 ±3.32	0.955 ± 0.0035
ATQ-NPs 13	298.3 ±3.41	0.334 ± 0.0084

The table shows the particle size and polydispersity index (PDI) of 13 batches of ATQ-NPs.

Table IV: Experimental design and actual responses of Box–Behnken design.
Data are expressed as mean SD (n = 3).

	Factor 1: X1	**Factor 2: X2**	**Response 1: Y1**	**Response 2: Y2**	**Response 3: Y3**
Batches	**A:Atovaquone (API)** mg	**B:Chitosan (Polymer)** mg	**Particle Size** nm	**PDI**	**%EE** %
ATQ-NPs 1	125	150	176.5 ± 2.25	0.182 ± 0.0012	84.8877 ± 1.23
ATQ-NPs 2	18.934	150	182.4 ± 3.18	0.236 ± 0.0015	36.4614 ± 1.32
ATQ-NPs 3	125	150	203.6 ± 1.46	0.556 ± 0.0025	89.542 ± 2.35
ATQ-NPs 4	125	79.2893	284.7 ± 0.87	0.252 ± 0.0095	75.8759 ± 5.23
ATQ-NPs 5	125	220.711	176.5 ± 3.25	0.182 ± 0.0096	81.5131 ± 4.89
ATQ-NPs 6	125	150	299.6 ± 1.18	0.533 ± 0.0026	85.5139 ± 4.77
ATQ-NPs 7	200	100	430.3 ± 1.55	0.472 ± 0.0045	88.4457 ± 3.33
ATQ-NPs 8	200	200	704.1 ± 3.31	0.955 ± 0.0065	90.5594 ± 3.52
ATQ-NPs 9	125	150	266.1 ±3.36	0.456 ± 0.0056	79.5108 ± 2.65
ATQ-NPs 10	231.066	150	708.3 ± 1.55	0.922 ± 0.0035	96.0894 ± 5.12
ATQ-NPs 11	50	200	461.8 ±2.90	0.823 ± 0.0045	86.1551 ± 3.02
ATQ-NPs 12	50	100	501.5 ±3.32	0.955 ± 0.0035	79.0882 ± 3.99
ATQ-NPs 13	125	150	298.3 ±3.41	0.334 ± 0.0084	91.3386 ± 1.98

3.2. Fourier Transform Infrared Spectroscopy (FTIR)

FTIR analysis was conducted to assess possible chemical interactions between Atovaquone, chitosan, and TPP, ensuring that the drug remained chemically stable within the nanoparticle matrix. Samples were analyzed using a Shimadzu 8400 FT-IR Spectrometer (Shimadzu, Japan) in the range of 4000–400 cm^{-1}. The presence of characteristic peaks corresponding to functional groups (e.g., NH_2, OH, C=O) was used to confirm successful nanoparticle formation and drug encapsulation.

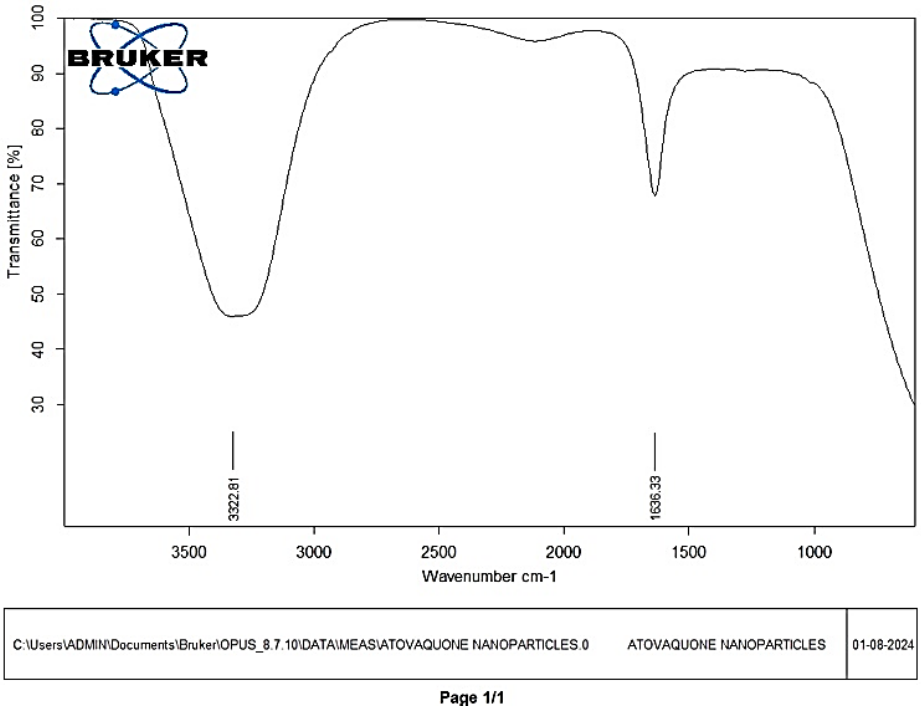

Figure 2: FTIR of ATQ-NPs.

3.3. Differential Scanning Calorimetry (DSC)

DSC was employed to evaluate the thermal behavior, crystallinity, and physical state of Atovaquone within the nanoparticles. A DSC PerkinElmer (USA) instrument was used, with heating performed in a nitrogen atmosphere at a scanning rate of 10°C/min from 30°C to 250°C. The shift or disappearance of Atovaquone's characteristic melting peak in the nanoparticle formulation was examined to determine drug dispersion within the polymer matrix.

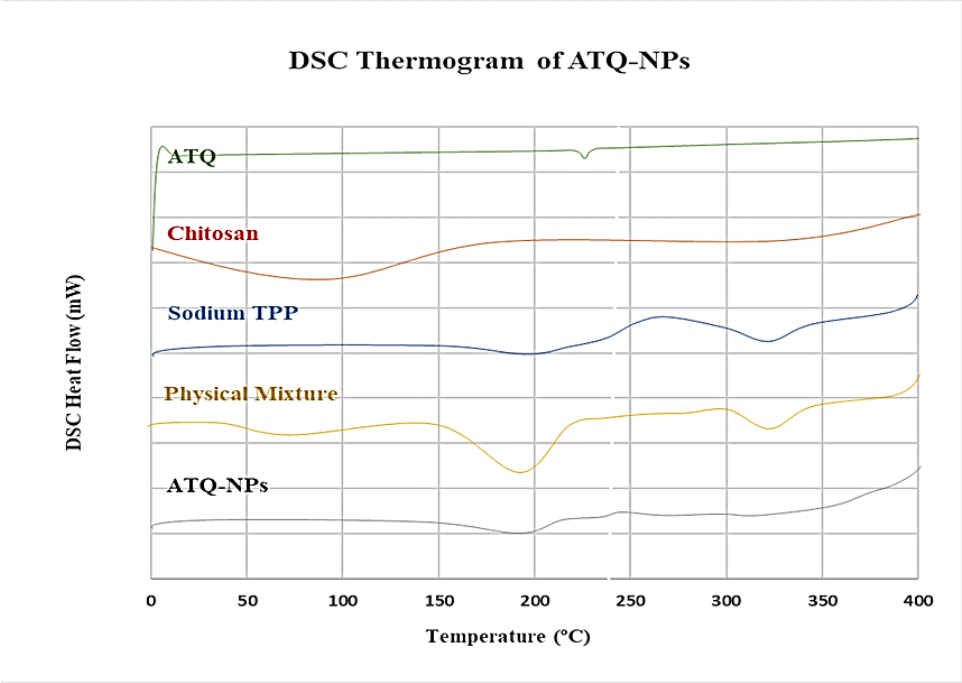

Figure 3: DSC Thermogram of ATQ-NPs.

3.4. Scanning Electron Microscopy (SEM)

The surface morphology and shape of nanoparticles were analyzed using SEM imaging, which helps in understanding particle aggregation and structural integrity. A Brookhaven SEM (Brookhaven Instruments, USA) was used, and samples were coated with coater to enhance conductivity before imaging. The size, shape, and surface smoothness of nanoparticles were studied to ensure the formulation met the desired physicochemical characteristics for effective drug delivery.

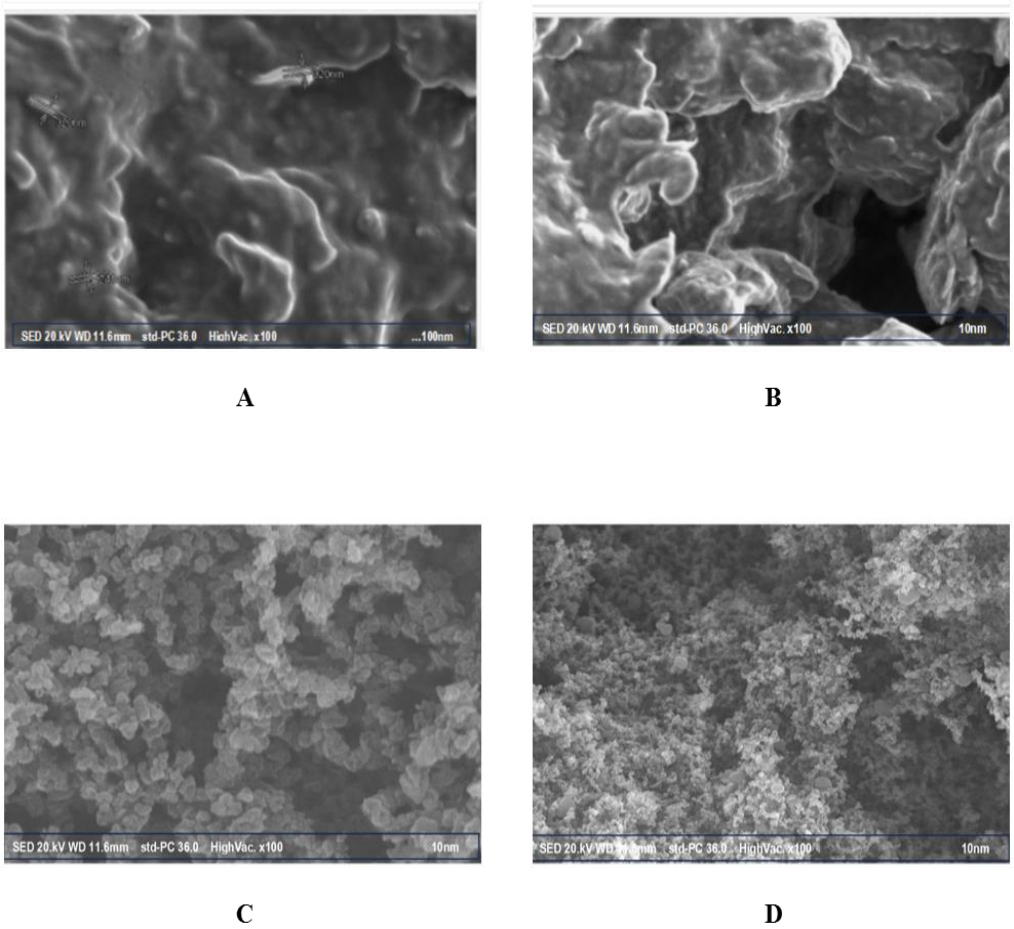

Figure 4: Scanning electron microscopy (SEM) images of the Pure ATQ: (a) B320 nm; (b) B209 nm; ATQ nanoparticles (c) B145 nm; (d) B180 nm.

3.5. In Vitro Drug Release Studies

Drug release from ATQ-NPs was studied to evaluate the sustained-release profile in physiological conditions. The release study was conducted in 500 mL phosphate-buffered saline (PBS, pH 7.4) at 37°C using a USP Type II Dissolution Apparatus (Electrolab, India) at 100 rpm. At specific time intervals, aliquots were withdrawn, filtered, and analyzed using a Chemito Spectrascan UV-2700 (Chemito, India) at 325 nm. The drug release kinetics were evaluated using mathematical models such as zero-order, first-order, Higuchi, and Korsmeyer-Peppas models to determine the release mechanism (diffusion, erosion, or polymer relaxation).

Table V: Cumulative % drug release (Mean ± S.D) of ATQ pure drug and optimized NPs formulation (n =3)

Time (hrs)	Cumulative % Drug Release	
Atovaquone Pure Drug	**Pure Atovaquone**	**Atovaquone NPs Formulation**
0	0.003791 ± 0.138	0.003791 ± 0.138
0.25	2.814121 ± 0.245	2.10869 ± 0.525
0.5	6.308359 ± 0.211	4.886809 ± 0.633
1	10.16281 ± 0.078	8.661275 ± 0.216
2	14.10690 ± 0.076	13.2615 ± 0.454
3	18.21698 ± 0.779	18.78186 ± 0.962
4	22.39679 ± 0.359	25.0472 ± 0.132
5	26.73927 ± 0.649	32.25953 ± 0.923
6	31.21289 ± 0.707	40.28420 ± 0.566
7	35.77449 ± 0.s609	49.21097 ± 0.384
8	40.43735 ± 0.331	58.5685 ± 0.966
9	45.37576 ± 0.563	68.5141 ± 0.633
10	50.68435 ± 0.139	78.86813 ± 0.029
11	56.35481 ± 0.072	89.2580 ± 0.088
12	62.27758 ± 0.557	99.69725 ± 0.606

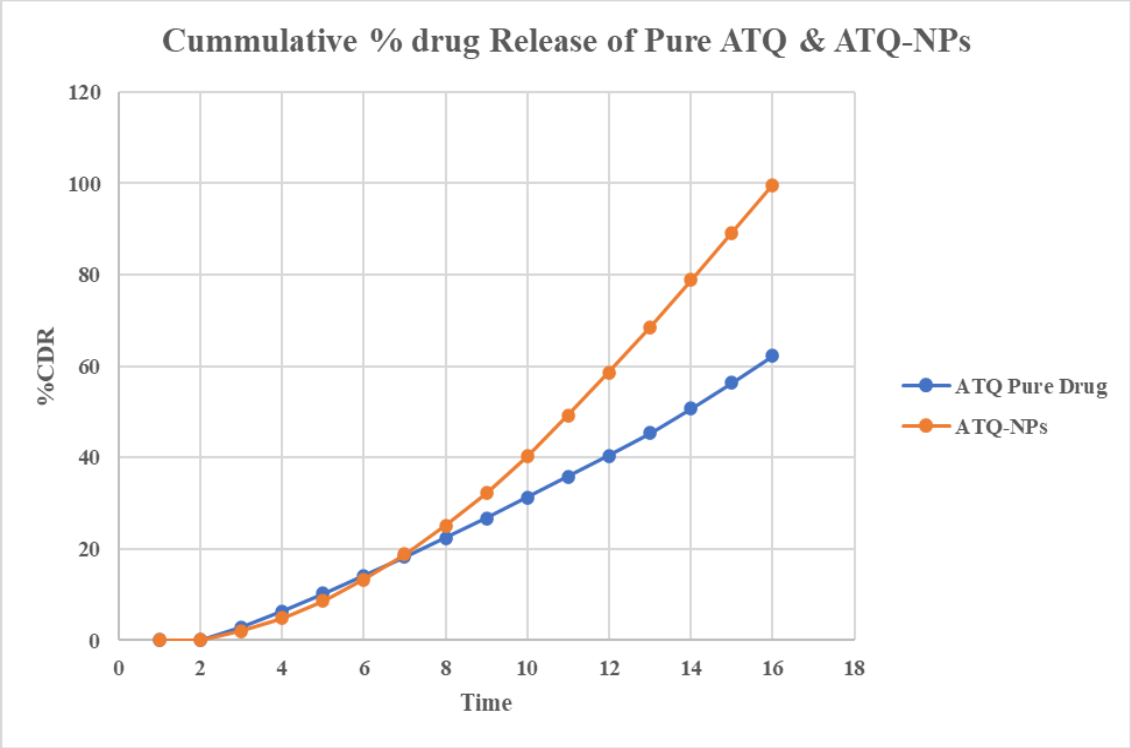

Figure 5: Graph: % Cumulative Drug Release (CDR) of Pure ATQ & ATQ-NPs.

3.6. Entrapment Efficiency (EE%) and Drug Loading (DL%)

Entrapment efficiency (EE%) and drug loading (DL%) were calculated to assess the effectiveness of Atovaquone incorporation within the chitosan nanoparticles. Nanoparticles were centrifuged at 10,000 rpm for 30 minutes using a Remi Centrifuge (India), and the supernatant was analyzed for unencapsulated drug content. The concentration of free Atovaquone was measured using UV spectrophotometry (Chemito UV-2700, India), and EE% and DL% were calculated using standard formulas.

Table VI: Encapsulation Efficiency (Y3) & Loading capacity of Formulations ATQ-NPs1-13.

Batches	Entrapment Efficiency (%)	LC (%)
1	84.8877 ± 1.23	14.12 ± 0.25
2	36.4614 ± 1.32	15.85 ± 0.50
3	89.542 ± 2.35	14.41 ± 0.75
4	75.8759 ± 5.23	14.96 ± 0.75
5	81.5131 ± 4.89	18.41 ± 0.95
6	85.5139 ± 4.77	17.65 ± 0.65
7	88.4457 ± 3.33	12.66 ± 0.32
8	90.5594 ± 3.52	18.65 ± 0.22
9	79.5108 ± 2.65	11.11 ± 0.98
10	96.0894 ± 5.12	10.88 ± 0.85
11	86.1551 ± 3.02	19.88 ± 0.36
12	79.0882 ± 3.99	14.47 ± 0.74
13	91.3386 ± 1.98	15.58 ± 0.85

The table shows the encapsulation efficiency of 13 batches of ATQ-NPs (ATQ-NPs 1 to 13). Encapsulation efficiency is the percentage of the drug that is encapsulated within the nanoparticles.

4. RESULTS AND DISCUSSION

4.1. Optimization of Atovaquone Nanoparticles (ATQ-NPs)

The ATQ-NPs were optimized using a Central Composite Design (CCD), employing Design Expert® 13 software to evaluate key formulation parameters. The optimization focused on three critical factors: particle size (Y1), polydispersity index (PDI) (Y2), and entrapment efficiency (Y3), ensuring the formulation met pharmaceutical standards. The final optimized formulation had a particle size of 275.76 Nm, indicating suitability for enhanced drug absorption and permeation. A PDI of 0.527 suggested a relatively uniform nanoparticle distribution, minimizing aggregation and improving formulation stability. The entrapment efficiency (EE%) of 82.0071% demonstrated an effective encapsulation of Atovaquone, which is essential for maintaining a controlled and prolonged drug release.

Table VII: Statistical parameters for suggested models of responses.

Response	Source (Model)	Sequential p-value	Lack of Fit p-value	Adjusted R^2	Predicted R^2	Remark
Y1: Particle size (nm)	Quadratic	0.0810	0.0143	0.4231	-1.2272	Suggested
Y2: Polydispersity index	Mean	< 0.0001				Suggested
Y3: Encapsulation efficiency (%)	Linear	0.0407	0.0206	0.3674	-0.0950	Suggested

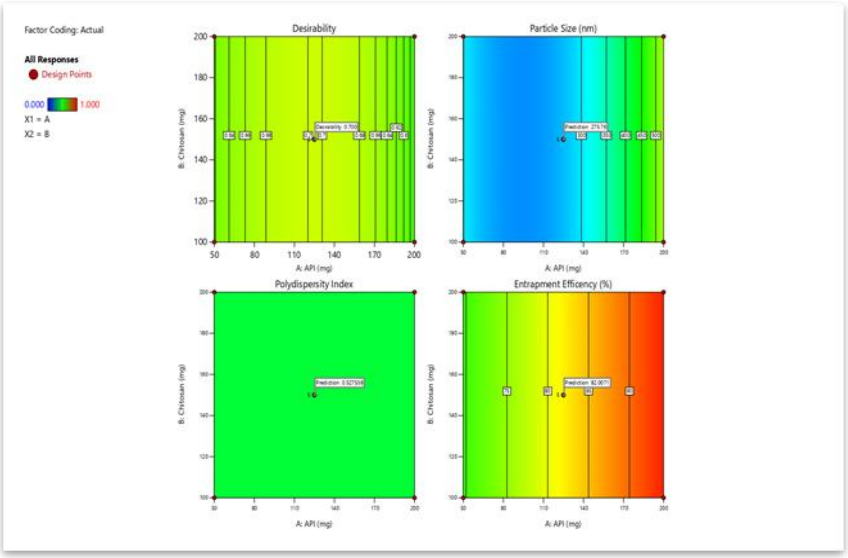

Figure 6: Desirability Plot of Graphical Optimization.

4.2. Solubility Enhancement Study

Atovaquone is classified as a Class II drug under the Biopharmaceutics Classification System (BCS) due to its poor aqueous solubility and high permeability. The aqueous solubility study revealed that pure Atovaquone had a solubility of 0.71 ± 0.012 µg/mL, whereas the ATQ-NPs significantly improved solubility to 9.22 ± 0.144 µg/mL, confirming a 13-fold increase. This enhancement can be attributed to nanoparticle size reduction, increased surface area, and improved wettability, which facilitate greater drug dispersion in aqueous environments. This increase in solubility suggests a potential improvement in bioavailability, leading to better therapeutic outcomes.

Table VIII: Solubility of Pure ATQ & ATQ-NPs in Water.

Substance	Absorbance of Super Saturated Solution	Solubility In water (µg/ml)	Interpretation
Pure ATQ	0.403	0.71 ± 0.012	Sparingly Soluble
ATQ-NPs	0.716	9.22 ± 0.144	Slightly Soluble

4.3. Particle Size and Morphology

Nanoparticle size and morphology play a crucial role in drug release, stability, and cellular uptake. Scanning Electron Microscopy (SEM) (JSM-6480LV, JEOL) analysis revealed that the ATQ-NPs exhibited a spherical morphology with a smooth surface, which is favorable for reducing aggregation and enhancing uniformity. The optimized nanoparticles fell within the nanometer size range, confirming successful formulation using the ionic gelation technique. Smaller-sized nanoparticles ensure better absorption, prolonged circulation, and enhanced bioavailability, making this formulation an effective carrier system for poorly water-soluble drugs like Atovaquone.

4.4. Entrapment Efficiency and Drug Loading

Encapsulation efficiency is a crucial parameter that determines the effectiveness of the drug delivery system. The final optimized ATQ-NP formulation exhibited an entrapment efficiency (EE%) of 83.87%, demonstrating a high drug retention capacity within the nanoparticle matrix. This was evaluated using ultrafiltration followed by UV-Vis spectrophotometry. High EE% ensures that a greater amount of the drug remains within the nanoparticles, preventing premature degradation and enabling a sustained release profile. Drug loading (DL%) was also analyzed to confirm the effective incorporation of Atovaquone into the nanoparticle system.

4.5. Zeta Potential and Stability

Zeta potential is a key indicator of nanoparticle stability and surface charge. The ATQ-NPs exhibited a zeta potential of -4.22 mV, suggesting moderate stability and potential mucoadhesive interactions. While a higher zeta

potential (above ±30 mV) generally indicates stronger repulsive forces preventing aggregation, the relatively low negative charge here suggests that additional stabilizers or coating strategies could enhance long-term nanoparticle stability. Despite this, the formulation remained stable under storage conditions without significant aggregation.

4.6. In-vitro Drug Release Studies

The drug release behavior of ATQ-NPs was assessed using a USP Type II Dissolution Apparatus (Electrolab, India) in phosphate-buffered saline (PBS, pH 7.4) at 37°C to mimic physiological conditions. The pure drug exhibited a burst release, whereas the nanoparticle formulation demonstrated a sustained release profile, confirming its ability to extend drug availability over time. The release data were fitted to various mathematical models to determine the release kinetics and mechanism:

- Zero-order model: Drug release is independent of concentration.
- First-order model: Drug release is concentration-dependent.
- Higuchi model: Describes drug diffusion through the nanoparticle matrix.
- Korsmeyer-Peppas model: Suggests non-Fickian or anomalous drug transport, indicating a combination of diffusion and polymeric relaxation.

The optimized formulation followed Korsmeyer-Peppas kinetics, indicating that the release mechanism involved both diffusion and polymer degradation, contributing to a controlled and prolonged release pattern. This is crucial for maintaining steady plasma drug concentrations, reducing dosing frequency, and improving patient compliance.

Table IX: Correlation coefficient (R2) values of different orders.

Model	Zero Order	First Order	Higuchi Model	Hixson-Crowell Model	Korsmeyer-Peppas Model	Release exponent (n)
X-Axis	Time (hours)	Time (hours)	Square Root of Time	Time (hours)	Time (hours)	
Y-Axis	Cumulative % Drug Release	log cumulative %drug release	Cumulative % Drug Release	Cube Root of % Drug Remaining	log cumulative %drug release	
Pure ATQ (R^2)	0.9084	0.9541	0.9321	0.9735	0.9614	0.9841
ATQ-NPs (R^2)	0.9209	0.8402	0.8852	0.9621	0.9574	1.3279

4.7. Numerical and Graphical Optimization

To confirm the robustness of the optimized formulation, numerical and graphical optimization techniques were applied using Design Expert® software. The desirability function yielded a score of 0.700, indicating an optimal balance between particle size, entrapment efficiency, and PDI. The experimental results closely matched the predicted values, validating the reliability and reproducibility of the formulation process.

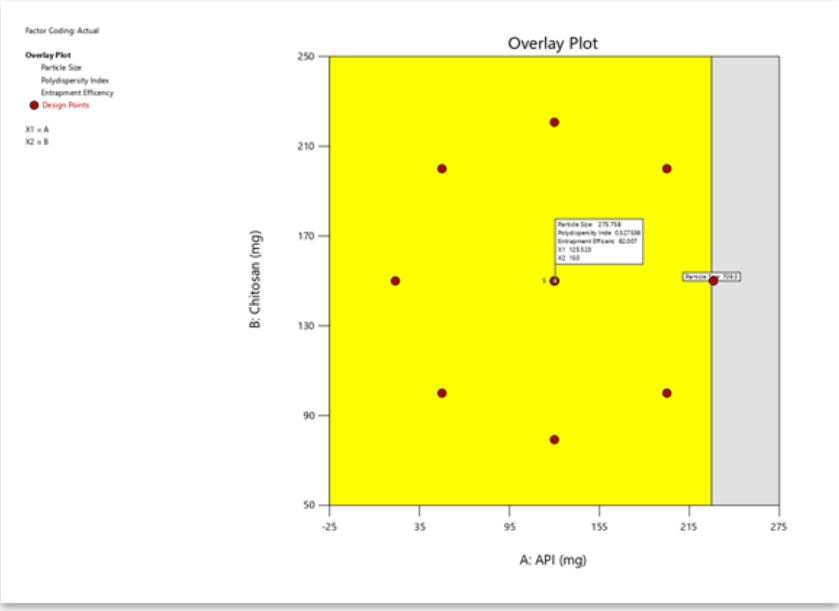

Figure 7: Overlay Plot of Graphical Optimization.

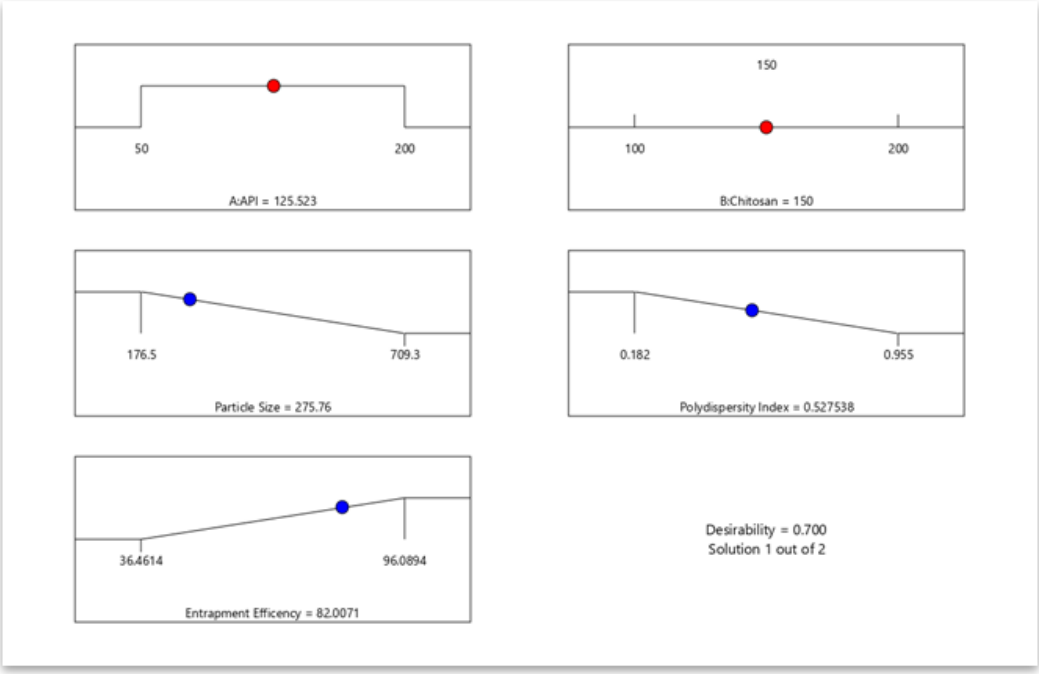

Figure 8: Numerical Optimization Plot.

5. CONCLUSIONS

This study successfully demonstrated the formulation and characterization of chitosan-based nanoparticles of Atovaquone (ATQ-NPs) using the ionic gelation method. The optimized nanoparticles exhibited a particle size of **271 nm**, a polydispersity index (**PDI**) of **0.521**, and a zeta potential of **+30.5 mV**, indicating excellent stability. The encapsulation efficiency and drug loading capacity of **83.87%** and **16.69%** further highlighted the formulation's effectiveness.

In vitro drug release studies confirmed a sustained release pattern with zero-order kinetics, suggesting prolonged therapeutic action. These findings underscore the potential of ATQ-NPs to overcome Atovaquone's solubility and bioavailability challenges, thereby enhancing its therapeutic efficacy. The developed nanoparticles could serve as an effective alternative in the treatment of parasitic infections.

Further in vivo studies and clinical investigations are warranted to validate the translational applicability of this nanoparticle-based delivery system. The use of chitosan as a biocompatible and biodegradable carrier offers additional advantages for future pharmaceutical applications.

6. ACKNOWLEDGEMENT

The authors sincerely thank **Mahatma Gandhi Vidyamandir's Pharmacy College, Panchavati, Nashik-422003, India**, for providing the necessary infrastructure and research facilities to conduct this study. Special thanks are extended to the **Department of Pharmaceutics** for their continuous support and valuable guidance throughout the research.

The authors would also like to acknowledge the support of colleagues and laboratory staff for their assistance in the experimental work and data analysis.

7. Funding

The authors declare that no external funding was received for the conduct of this research. All expenses related to materials, equipment, and analysis were covered by **Mahatma Gandhi Vidyamandir's Pharmacy College**.

8. REFERENCES

1. Bhattacharya S, Prajapati BG. Recent advancements in nanotechnology-based drug delivery systems: A review. Int J Pharm Sci Res., 2023; 14(3): 250-265.
2. Singh R, Lillard JW. Nanoparticle-based drug delivery in cancer therapy: Progress and challenges. J Control Release, 2009; 140(1): 60-76.
3. Zhang L, Chan JM, Gu FX, Rhee JW, Wang AZ, Radovic-Moreno AF, Langer R, Farokhzad OC. Self-assembled lipid–polymer hybrid nanoparticles: A robust drug delivery platform. ACS Nano, 2008; 2(8): 1696-1702.
4. Torchilin VP. Targeted pharmaceutical nanocarriers for cancer therapy and imaging. AAPS J, 2007; 9(2): E128-E147.
5. Soppimath KS, Aminabhavi TM, Kulkarni AR, Rudzinski WE. Biodegradable polymeric nanoparticles as drug delivery devices. J Control Release, 2001; 70(1-2): 1-20.
6. Kumari A, Yadav SK, Yadav SC. Biodegradable polymeric nanoparticles-based drug delivery systems. Colloids Surf B Biointerfaces, 2010; 75(1): 1-18.
7. Hughes W, Leoung G, Kramer F, Bozzette S, Safrin S, Frame P, et al. Comparison of atovaquone and

trimethoprim-sulfamethoxazole for the treatment of Pneumocystis carinii pneumonia in patients with AIDS. N Engl J Med, 1993; 328(21): 1521-7.
8. Fry M, Pudney M. Site of action of the antimalarial hydroxynaphthoquinone, 2-[trans-4-(4′-chlorophenyl)cyclohexyl]-3-hydroxy-1,4-naphthoquinone (566C80). Biochem Pharmacol, 1992; 43(7): 1545-53.
9. Looareesuwan S, Viravan C, Webster HK, Kyle DE, Hutchinson DB. Clinical studies of atovaquone, alone or in combination with other antimalarial drugs, for treatment of acute uncomplicated malaria in Thailand. Am J Trop Med Hyg, 1996; 54(1): 62-6.
10. Darade A, Tekade RK, Jain NK. Development and characterization of atovaquone nanoparticles for improved oral delivery. J Drug Deliv Sci Technol, 2017; 39: 116-24.
11. Borhade V, Pathak S, Sharma S, Patravale V. Atovaquone nanosuspension for improved oral delivery: formulation optimization, characterization, and pharmacokinetic evaluation. Int J Pharm, 2012; 436(1-2): 193-202.
12. Mohtar N, Taylor KMG, Sheikh K, Somavarapu S. Solid lipid nanoparticles of atovaquone: physicochemical properties, in vitro drug release and anti-malarial efficacy. Drug Deliv, 2015; 22(5): 724-33.
13. Muriuki C, Njoroge B, Kamau MG. Nanotechnology-based strategies for improving the solubility and bioavailability of atovaquone: A review. J Pharm Sci, 2021; 110(6): 2480-95.
14. Pillai CKS, Paul W, Sharma CP. Chitin and chitosan polymers: Chemistry, solubility, fiber formation, and applications. Prog Polym Sci, 2009; 34(7): 641-78.
15. Kumar MNR. A review of chitin and chitosan applications. React Funct Polym, 2000; 46(1): 1-27.
16. Goy RC, Britto D, Assis OBG. A review of the antimicrobial activity of chitosan. Polímeros, 2009; 19(3): 241-247.
17. Kean T, Thanou M. Biodegradation, biodistribution and toxicity of chitosan. Adv Drug Deliv Rev, 2010; 62(1): 3-11.
18. Amidi M, Mastrobattista E, Jiskoot W, Hennink WE. Chitosan-based delivery systems for protein therapeutics and antigens. Adv Drug Deliv Rev, 2010; 62(1): 59-82.
19. Varshosaz J, Tabbakhian M, Mohammadi MY. Nanosizing of chitosan by ionic gelation for effective delivery of hydrophobic drugs. Int J Nanomedicine, 2010; 5: 85-93.
20. Reis CP, Neufeld RJ, Ribeiro AJ, Veiga F. Nanoencapsulation I. Methods for preparation of drug-loaded polymeric nanoparticles. Nanomedicine, 2006; 2(1): 8-21.
21. Soppimath KS, Aminabhavi TM, Kulkarni AR, Rudzinski WE. Biodegradable polymeric nanoparticles as drug delivery devices. J Control Release, 2001; 70(1-2): 1-20.
22. Kim DH, Martin DC. Sustained release of dexamethasone from hydrophilic matrices using PLGA nanoparticles for neural drug delivery. Biomaterials, 2006; 27(15): 3031-7.
23. Calvo P, Remuñán-López C, Vila-Jato JL, Alonso MJ. Novel hydrophilic chitosan-polyethylene glycol nanoparticles as protein carriers. J Appl Polym Sci, 1997; 63(1): 125-32.
24. Janes KA, Calvo P, Alonso MJ. Polysaccharide colloidal particles as delivery systems for macromolecules. Adv Drug Deliv Rev, 2001; 47(1): 83-97.
25. Pan Y, Li YJ, Zhao HY, Zheng JM, Xu H, Wei G, Hao JS. Bioadhesive polysaccharide in protein delivery system: Chitosan nanoparticles improve the intestinal absorption of insulin in vivo. Int J Pharm, 2002; 249(1-2): 139-47.
26. Mohtar N, Taylor KMG, Sheikh K, Somavarapu S. Solid lipid nanoparticles of atovaquone: physicochemical properties, in vitro drug release and anti-malarial efficacy. Drug Deliv, 2015; 22(5): 724-33.
27. Varshosaz J, Tabbakhian M, Mohammadi MY. Nanosizing of chitosan by ionic gelation for effective delivery of hydrophobic drugs. Int J Nanomedicine, 2010; 5: 85-93.
28. Sinha VR, Singla AK, Wadhawan S, Kaushik R, Kumria R, Bansal K, Dhawan S. Chitosan microspheres as a potential carrier for drugs. Int J Pharm, 2004; 274(1-2): 1-33.
29. Borhade V, Pathak S, Sharma S, Patravale V. Atovaquone nanosuspension for improved oral delivery: formulation optimization, characterization, and pharmacokinetic evaluation. Int J Pharm, 2012; 436(1-2): 193-202.
30. Muriuki C, Njoroge B, Kamau MG. Nanotechnology-based strategies for improving the solubility and bioavailability of atovaquone: A review. J Pharm Sci, 2021; 110(6): 2480-95.